nature communications

Article

https://doi.org/10.1038/s41467-024-52697-5

"Pink power"—the importance of coralline algal beds in the oceanic carbon cycle

Received: 2 April 2024

Accepted: 18 September 2024

Published online: 27 September 2024

Check for updates

Nadine Schubert[1] ✉, Fernando Tuya[2], Viviana Peña[3], Paulo A. Horta[4], Vinícius W. Salazar[4,17], Pedro Neves[1,5], Cláudia Ribeiro[1,6], Francisco Otero-Ferrer[2,7], Fernando Espino[2], Kathryn Schoenrock[8], Federica Ragazzola[9,10], Irene Olivé[11], Thalassia Giaccone[10,12], Matteo Nannini[9], M. Cristina Mangano[10,13], Gianluca Sará[10,14], Francesco Paolo Mancuso[10,14], Mario Francesco Tantillo[14], Mar Bosch-Belmar[10,14], Sophie Martin[15], Line Le Gall[16], Rui Santos[1] & João Silva[1]

Current evidence suggests that macroalgal-dominated habitats are important contributors to the oceanic carbon cycle, though the role of those formed by calcifiers remains controversial. Globally distributed coralline algal beds, built by pink coloured rhodoliths and maerl, cover extensive coastal shelf areas of the planet, but scarce information on their productivity, net carbon flux dynamics and carbonate deposits hampers assessing their contribution to the overall oceanic carbon cycle. Here, our data, covering large bathymetrical (2–51 m) and geographical ranges (53°N–27°S), show that coralline algal beds are highly productive habitats that can express substantial carbon uptake rates (28–1347 g C m^{-2}), which vary in function of light availability and species composition and exceed reported estimates for other major macroalgal habitats. This high productivity, together with their substantial carbonate deposits (0.4–38 kilotons), renders coralline algal beds as highly relevant contributors to the present and future oceanic carbon cycle.

The important role of the oceans in the global carbon cycle is well established[1], determined by the solubility and the biological pump that regulate the partitioning of carbon between the ocean and the atmosphere[2]. The biological pump combines the carbon pools from both the soft tissue pump and the carbonate pump, linking the conversion of dissolved inorganic carbon (DIC) to organic carbon by autotrophic net primary production (NPP) and the precipitation of $CaCO_3$ by calcifying organisms, respectively[2]. Hence, NPP is a major driver of carbon cycling through the biological pump, and quantifying the sources, patterns and drivers is fundamental. In this context, Pessarrodona et al[3,4]. recently pointed out that coastal carbon fluxes are inadequately represented in the global carbon budget, as many uncertainties remain, mostly related to the quantitative importance of the carbon uptake by marine vegetated habitats, in comparison with other primary producers (e.g., phytoplankton). Over the last few years, efforts have increased to elucidate the magnitude of carbon uptake linked to NPP in these habitats and to identify patterns and potential drivers[5–7]. Recent data compilations[8] confirmed that macroalgal-dominated habitats are among the largest and most productive coastal vegetated ecosystems, comparable or even more productive than oceanic phytoplankton and some terrestrial ecosystems[3,9].

While the significant contribution of non-calcareous macroalgal habitats to oceanic carbon uptake has recently been acknowledged, the carbon capture potential of habitats created by calcifiers remains controversial[10]. The common assumption is that calcifiers and the habitats they build (e.g., coral reefs, calcareous algal beds) represent a source of atmospheric CO_2 via the process of calcification[10,11]. Indeed, marine shallow benthic carbonate production has been associated with a net CO_2 evasion to the atmosphere, as the precipitation of calcium carbonate ($CaCO_3$) is a process that releases CO_2, while its dissolution has the opposite effect[12,13]. Yet, in habitats built by photosynthetic calcifiers, carbon flux dynamics are driven by the

A full list of affiliations appears at the end of the paper. ✉e-mail: nadine_schubert@hotmail.com

co-deposition of organic (soft tissue) and inorganic (in form of $CaCO_3$) carbon, which have opposing effects on the magnitude and direction of a habitat's net carbon fluxes. Thus, the ratio of organic to inorganic carbon production has been suggested as a controlling factor for carbon sink/source potential of habitats built by calcifiers, such as coral reefs[14]. In this context, coral reefs are generally assumed to be carbon sources, as earlier estimates suggested that the daily net organic carbon production in these systems is ~0, due to net photosynthetic carbon assimilation during the day being offset by carbon release due to nighttime respiration[15]. However, increasing evidence indicates that net organic carbon production in reefs is highly variable and can be >0, off-setting the CO_2 release due to calcification[16–18]. Similar findings have been reported for seagrass ecosystems with a high proportion of associated calcareous macroalgae[10,19], and for communities dominated by coralline algae[20].

In contrast to coral reefs, where assessments of the magnitude and direction of associated carbon fluxes have been carried out since the 90 s, research efforts have been extremely limited for coralline algal beds. These habitats are built by usually pink coloured free-living non-geniculate coralline algae, i.e. rhodoliths (nucleated forms) and maerl (non-nucleated forms). They represent a major marine benthic habitat, with an estimated global area of 4.12 million km^2[21], which is by far larger than the global estimates for other macroalgal-dominated habitats[9,22]. Yet, studies on the productivity and associated carbon sink-source dynamics of coralline algal beds are extremely limited, in both numbers and geographical scale, which is a crucial obstacle for obtaining meaningful global estimates. Currently, available datasets are restricted to temperate and cold-temperate coralline algal beds, suggesting that these habitats are mostly net heterotrophic throughout the year, i.e. carbon release is higher than its uptake[23–25], though slight autotrophy has been reported in a shallow bed during spring[26]. Consequently, in recent comparisons of productivity and associated carbon uptake of different macroalgal habitats, coralline algal beds rank among the habitats with the lowest values[3,9].

As outlined above, for the quantification of the net carbon uptake capacity of calcifying habitats, such as coralline algal beds, both net organic carbon metabolism and carbonate dynamics (inorganic carbon cycling) must be considered. In this context, the available information shows that in rhodoliths and maerl (hereafter using the term rhodoliths for both), the ratio of net photosynthesis to calcification varies depending on species and environmental conditions[23,27,28]. This would suggest considerable variability in productivity-associated carbon flux dynamics depending on site, season and/or rhodolith-community composition. When considering coralline algal beds at an ecosystem level, this ratio can also vary depending on the type and abundance of the associated community (e.g., fauna, flora, calcifiers, non-calcifiers), which contribute differentially to the carbon fluxes[24,29].

Furthermore, coralline algal beds often contain substantial carbonate deposits (e.g., 200 Gt $CaCO_3$ on the Brazilian coastal shelf alone[30,31]), as shallow-water (< 100 m) benthic carbonate production leads foremost to carbonate accumulation with little dissolution[13]. These deposits are frequently stable for millennia[32], and represent a significant carbon sink, though they are considered relevant only at long-term (i.e., geological) timescales[33,34]. Yet, their relevance for short-term habitat-associated carbon fluxes may increase due to ocean acidification that results in a decline in the calcium carbonate saturation state of seawater[35], and a consequent increase of dissolution of the carbonate deposits, as shown experimentally for dead rhodoliths[36], and reported for coral reefs and carbonate sediments[37–39]. From a biogeochemical perspective, an increase in carbonate dissolution would increase seawater alkalinity and cause a CO_2 drawdown associated with these habitats[13].

Information regarding contemporary carbon fluxes (associated to net organic carbon metabolism and carbonate dynamics) and the extent of their carbonate deposits, are both highly relevant for present-day assessments and future projections of the role of coralline algal beds in the oceanic carbon cycle. For the former, a bottom up approach can be used, scaling up from individual-level physiological processes to the population level. This approach has been widely applied in macroalgal-dominated habitats, including coralline algal beds[23,29,40–43], and in coral reefs[44,45]. In coralline algal beds, and similar to studies in coral reefs[16,46], it involves a budgeting approach, considering (i) net primary productivity, i.e. the balance between organic carbon production and consumption, and (ii) the balance between calcium carbonate precipitation (CO_2 release) and dissolution (CO_2 removal).

Given the information outlined above, it is reasonable to assume that coralline algal beds might play an important, yet so far not considered, role in the oceanic carbon cycle. In this study, we investigated this question, by assessing (i) the magnitude, direction and drivers of carbon fluxes associated to the productivity of coralline algal beds and their geographical and species-specific variability, and (ii) the amount of carbonate accumulated in these habitats and its dissolution rates. For this, net primary and carbonate production rates of individual rhodolith species from the sampled coralline algal beds were quantified at different light levels. In addition, the dissolution rates of dead algal nodules/thalli were determined, as these can represent a significant proportion of the rhodolith standing stock in these habitats. The obtained rates were combined with information of the respective standing stocks (live and dead rhodoliths) and in situ light field and variability data, to obtain daily estimates of net coralline algal productivity (living rhodolith community), carbonate dissolution rates (dead algal nodules/thalli) and the resulting net carbon uptake/release. Moreover, considering the aforementioned standing stocks, we estimated the amount of carbonate accumulated in the beds.

Results

The daily integrated net primary productivity (NPP) of species that inhabit and dominate different Atlantic and Mediterranean coralline algal beds showed that they were net autotrophic, except the rhodoliths from the deepest bed (Sicily, 51 m) that showed slight net heterotrophy (Fig. 1a, Supplementary Table 1). The estimates of both NPP and daily integrated net carbonate production (NCP) were highly correlated ($R^2 = 0.97$), even though they were quite variable among and within sites (Fig. 1b, c). Regardless of the species, light availability explained 61% and 63% of variation in NPP and NCP, respectively (Supplementary Fig. 1). NPP and NCP increased with light availability (Fig. 1a, b), while site-specific temperatures hardly contributed to differences in rhodolith productivity (Supplementary Fig. 1).

The strong influence of local light conditions on rhodolith productivity was also supported by comparing estimates of the same species (*Phymatolithon* sp.) from four coralline algal beds in the Lusitanian province. Both, NPP and NCP of this species varied strongly among sites that differed in depth and, consequently, in the daily light exposure, with rhodoliths from the shallowest (Arguineguin) and deepest bed (Porto Santo) expressing the highest and lowest productivity, respectively (Fig. 2a).

Additionally, comparison of the productivity estimates from multiple species, inhabiting the same coralline algal bed, indicated that species-specific productivity may contribute to the observed variation. This is exemplified in the Arvoredo bed (southern Brazil), where there were significant differences in productivity among the species dominating the community (Fig. 2b, Supplementary Table 1).

Rhodolith productivity per m^2 of coralline algal bed (NPP_P, NPC_P), showed a similar pattern relative to the biomass-specific productivity (Fig. 3a, Table 1), despite differences in the biomass of living rhodoliths in the coralline algal beds, which ranged from 2.5 to 29 kg m^{-2} (Table 2). The daily NPP_P indicated that the deepest bed (Sicily) was slightly net heterotrophic, while coralline algal beds with the highest in situ light availability (Arvoredo, Arguineguin, Taranto), expressed the highest

https://doi.org/10.1038/s41467-024-52697-5

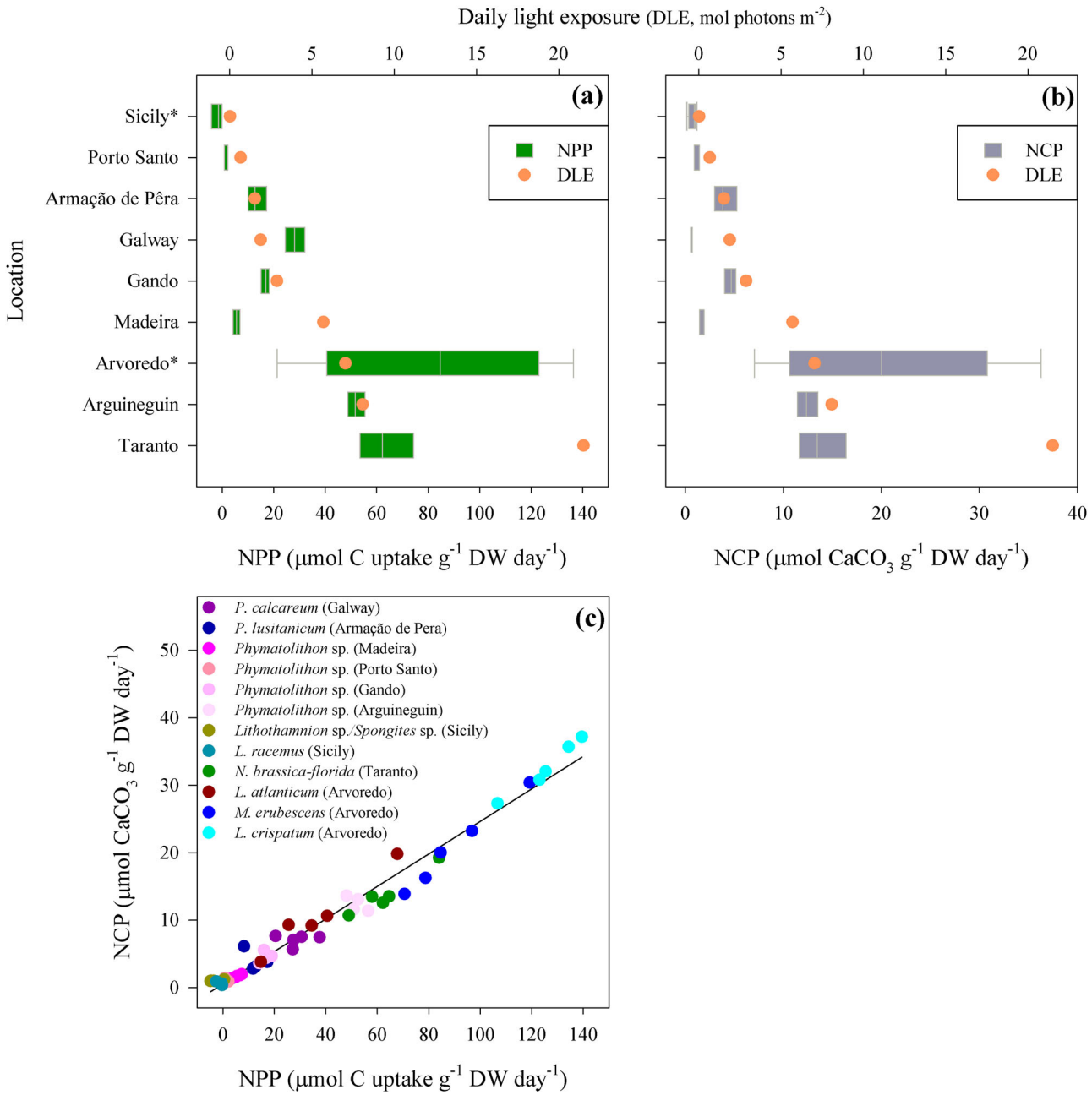

Fig. 1 | Daily net productivity of rhodoliths from Atlantic and Mediterranean coralline algal beds. a Biomass-specific daily net primary productivity (NPP, expressed as carbon uptake) and (**b**) daily net carbonate production (NCP) and the corresponding daily light exposure (DLE). Box plots show the median (gray line), the box ends indicate the upper and lower quartiles and the box whiskers extend to the maxima and minima of each sample (excluding the outliers) [$n = 5$ per location, except for *multispecific rhodolith populations in Sicily ($n = 10$) and Arvoredo ($n = 15$)]. **c** Linear correlation between NPP and NCP ($y = 0.559 + 0.241\,x$, $R^2 = 0.97$).

productivity (Fig. 3a, Table 1). The highest estimate of NPP_P and NCP_P was found in the Brazilian bed, about twice as high as the other two most productive beds (Fig. 3a, Table 1).

Most of the rhodolith populations exhibited a NPP_P:NCP_P ratio > 1 (Table 1). Hence, the resulting net carbon fluxes, based on primary productivity and discounting for CO_2 release during carbonate production, indicated that the majority of the studied coralline algal beds were net autotrophic during the summer season, expressing net carbon uptake rates ranging from 26 mmol to 1.2 mol C m^{-2} day^{-1} (Fig. 3b, Table 1). The exception was the deepest bed in Sicily (51 m), which was net heterotrophic (NPP < 0) and expressed a slight net C release, while the beds with the highest light availability exhibited the highest carbon uptake rates.

Furthermore, a large variation was also found among coralline algal beds regarding their living rhodolith biomass, the ratio between living:dead rhodoliths, and the amounts of $CaCO_3$ accumulated in the beds. Living rhodolith biomass was site-specific (Fig. 3c) and the $CaCO_3$ content (per dry weight) of these rhodoliths varied from 89–98% (Table 2). Discounting for the latter and considering both components, living and dead rhodoliths, the resulting amount of $CaCO_3$ accumulated in the coralline algal beds also exhibited a large variability, ranging between 4 and 43 kg m^{-2} (Fig. 3d, Table 2). Thus, based on available information of the area of the studied coralline algal beds, they contain between 450 tons to 38 kilotons of $CaCO_3$ (Table 2).

https://doi.org/10.1038/s41467-024-52697-5

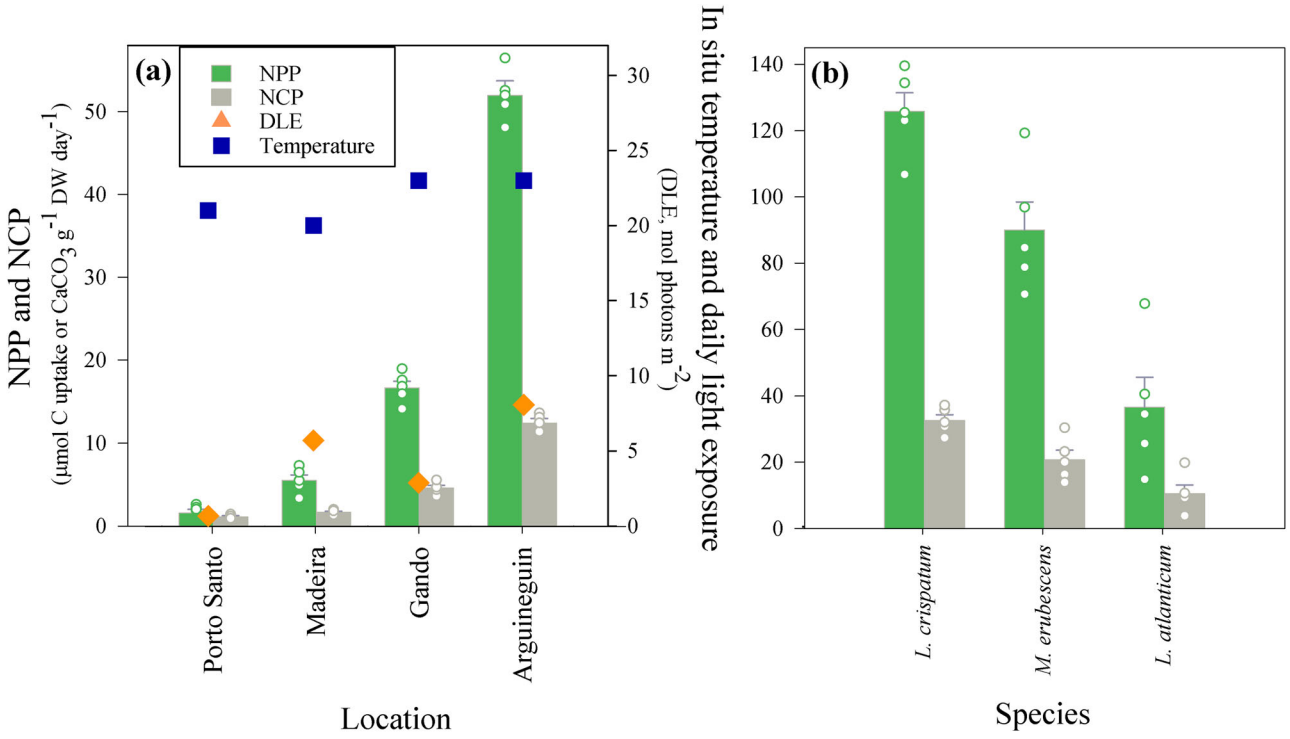

Fig. 2 | Variability of biomass-specific daily rhodolith net primary productivity (NPP) and net carbonate production (NCP). a Differences in productivity of *Phymatolithon* sp. from coralline algal beds in the Lusitanian province (14–33 m depth, $n = 5$ per location), under varying environmental conditions (one-way ANOVA; NPP, $F = 192.5$, $p < 0.0001$; NCP, $F = 175.8$, $p < 0.0001$), and (**b**) differences in productivity among multiple species from a coralline algal bed in Arvoredo, Brazil (8 m depth, $n = 5$ per species) (one-way ANOVA; NPP, $F = 33.0$, $p < 0.0001$; NCP, $F = 20.1$, $p = 0.00015$). Bars represent mean ± SE.

Moreover, the determined slow dissolution rates of the dead algal thalli (Supplementary Table 1), in conjunction with the standing stock of this component in the beds, indicated that its contribution to the net C uptake was neglectable in some beds, but could increase it in other beds. For example, in the Gando bed, which contains a rather large quantity of dead rhodoliths (24 kg m^{-2}), the dissolution of this component would result in an estimated increase in the daily net C uptake by ~12% (Table 1).

Discussion

Our data, obtained across a broad geographical scale, shows that coralline algal beds can be highly productive marine habitats, expressing high carbon uptake rates, and that they can accumulate substantial amounts of $CaCO_3$.

Currently, available information suggests that coralline algal beds exhibit a low net productivity when compared to other macroalgal-dominated habitats[3,9]. Yet, this is related to the extremely limited number of studies that have been focused so far solely on temperate and cold-temperate beds, which were reported to be mostly net heterotrophic[23–25]. By expanding the number of datasets of coralline algal beds to include a large latitudinal and bathymetric range, our estimates indicate that the productivity of these habitats, and their associated net carbon uptake, is currently underestimated. Daily summer estimates of NPP_P and NCP_P ranged between 0.6 and ~20 g C uptake m^{-2} day^{-1} (except for the deepest bed in Sicily that exhibited a slight net carbon release of 0.06 g C m^{-2} day^{-1}) and between 0.2 and 35 g $CaCO_3$ production m^{-2}, respectively. When extrapolating these data to seasonal productivity, the net carbon uptake due to net primary productivity during summer ranged between 50 and 1783 g C m^{-2} (except for the Sicilian bed, with net release of 6 g C m^{-2}). This carbon uptake was partially offset by the respective carbonate production, but still presented substantial values between 28 and 1347 g C uptake m^{-2}.

When comparing our estimates with recently compiled annual productivity data sets of other macroalgal habitats[9], it becomes clear that the productivity of coralline algal beds is currently underestimated (Fig. 4). The mean summer productivity per area (not extrapolated to annual values due to seasonal variability that would likely lead to an overestimation) is within a similar range, or even exceeding, the annual values reported for other seaweed habitats (Fig. 4a). Likewise, considering the substantial global area covered by coralline algal beds[21], the carbon uptake associated to summer production exceeds the values reported for other macroalgal habitats at a global scale[9] (Fig. 4b).

When comparing the estimated daily productivity of coralline algal beds with that reported for other calcifiers and the habitats they create, we found that the former can achieve higher values (Table 3). The higher productivity compared to other coralline algae (e.g., CCAs) is likely due to the high rhodolith density and the great variety of complex rhodolith morphologies, which increase their photosynthetic surface area[47]. The higher estimates of daily primary (organic carbon) production of coralline algal beds are accompanied by daily carbonate production rates similar to those found in other calcifiers, resulting in NPP:NCP > 1 for most of the beds (Table 3). Lower values of organic to inorganic carbon production (NPP:NCP < 1) are often reported for coral reefs, driving a normally low carbon uptake, a fact that led to the general assumption that these habitats are sources of atmospheric CO_2, rather than sinks[20,48]. On the other hand, the elevated NPP of coralline algal beds leads to a daily net carbon drawdown, despite their substantial carbonate production (Table 3). Hence, our results show that high carbonate production does not preclude net carbon uptake and confirm that the relative importance of the organic versus inorganic carbon cycle is a strong driver for the carbon sink/source duality in these habitats, as it has long been suggested for coral reefs[14,18]. Still, our estimates do not take into account the contribution of the associated community to productivity-related carbon fluxes (as is the case

https://doi.org/10.1038/s41467-024-52697-5

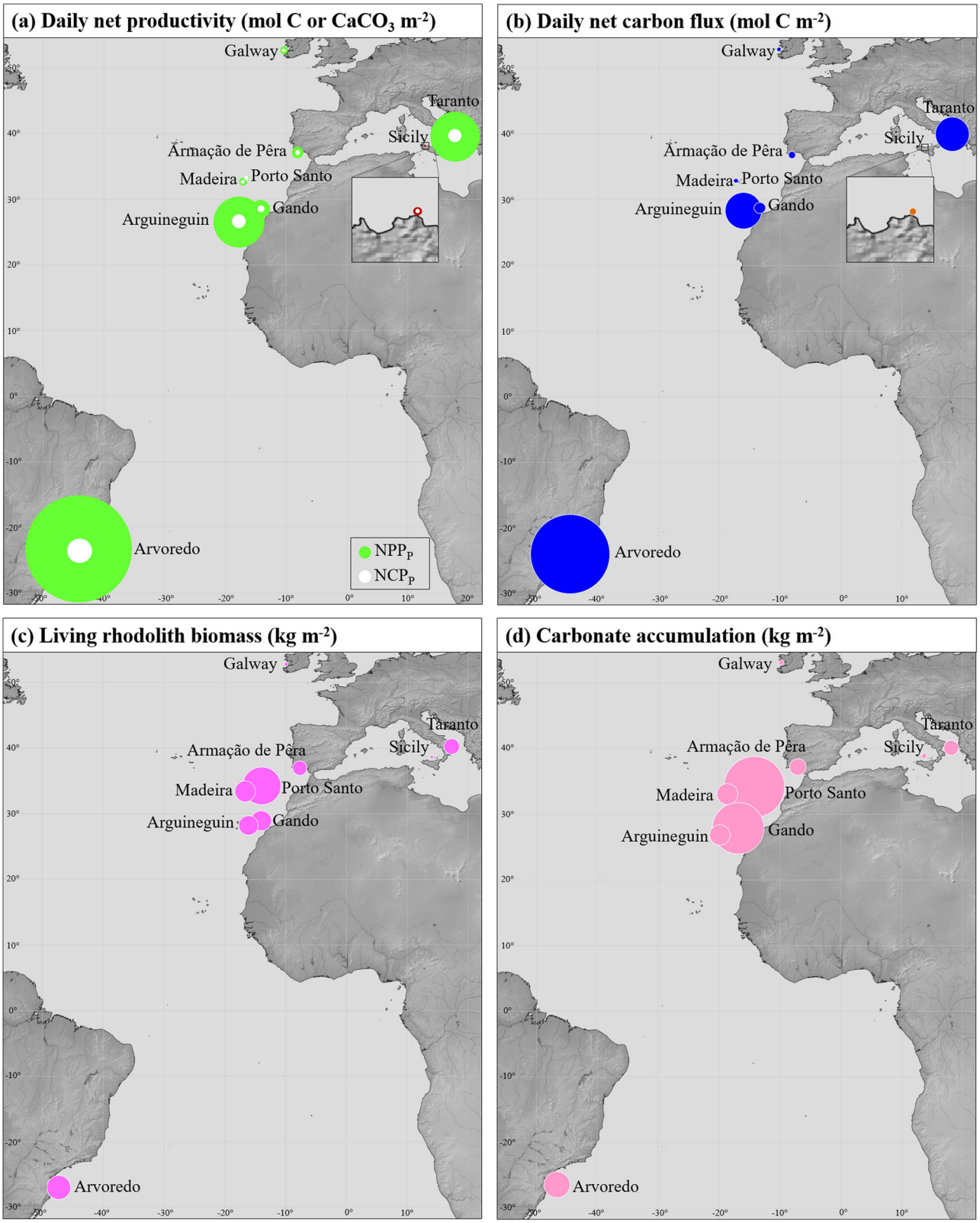

Fig. 3 | Relative comparison of the productivity and biomass/$CaCO_3$ standing stocks of Atlantic and Mediterranean coralline algal beds. a Daily net primary productivity (green- net C uptake, dark red- net C release) and net carbonate production (white) of rhodolith populations, and (**b**) the resulting daily net carbon flux (mol C m^{-2}; blue- net C uptake, orange- net C release). Inlet picture in (**a**, **b**) highlights enlarged (20 x) productivity and carbon flux of Sicilian bed. **c** Living rhodolith biomass and (d) $CaCO_3$ accumulated in the beds. For data, see Tables 1 and 2.

https://doi.org/10.1038/s41467-024-52697-5

Table 1 | Summary of mean (± SD) productivity of Atlantic and Mediterranean coralline algal beds, the resulting net DIC fluxes (negative- C uptake, positive- C release) and daily integrated carbonate dissolution rates of dead rhodoliths and estimated associated CO_2 flux (Ψ = 0.6 mol CO_2 per mol $CaCO_3$ dissolved[63,64])

Site	NPP_P (mmol C uptake m^{-2} day^{-1})	NCP_P (mmol $CaCO_3$ m^{-2} day^{-1})	Net DIC flux (mmol C m^{-2} day^{-1})	NPP_P:NCP_P	$CaCO_3$ dissolution (mmol m^{-2} day^{-1})	CO_2 flux due to dissolution (mmol m^{-2} day^{-1})
Galway	89.9 (±19.5)	22.2 (±2.5)	-86.6 (±14.2)	4.2 (±0.6)	1.2 (±0.8)	-0.75 (±0.5)
Armação de Pêra	148.6 (±42.7)	44.8 (±14.5)	-112.4 (±25.2)	3.6 (±1.3)	1.2 (±0.4)	-0.71 (±0.2)
Porto Santo	46.0 (±21.4)	33.9 (±10.3)	-25.9 (±15.7)	1.6 (±1.0)	12.8 (±1.4)	-7.7 (±0.8)
Madeira	86.2 (±23.7)	26.4 (±3.9)	-75.6 (±21.9)	3.2 (±0.5)	0.6 (±0.4)	-0.35 (±0.2)
Gando	256.9 (±27.8)	70.8 (±10.7)	-176.9 (±22.4)	3.7 (±0.5)	35.9 (±14.8)	-21.6 (±8.9)
Arguineguín	768.9 (±51.9)	180.7 (±16.4)	-574.9 (±61.0)	4.2 (±0.6)	3.3 (±1.4)	-2.0 (±0.8)
Taranto	745.1 (±151.3)	177.1 (±36.0)	-535.6 (±99.8)	4.6 (±0.3)	-	-
Sicily*	-5.2	1.9	5.6	-2.7	1.7 (±0.3)	-1.01 (±0.2)
Arvoredo*	1650.9	349.3	-1247.0	4.7	22.6 (±11.5)	-13.6 (±6.9)

*Mean (NPP_P:NCP_P) or sum of the productivity of a multiple-species population.

Table 2 | Summary of standing stocks of Atlantic and Mediterranean coralline algal beds, including biomass and carbonate content of living rhodoliths, ratios of live:dead, and the amount of carbonate accumulated (per m^2 and per bed)

Site	Rhodoliths (kg DW m^{-2})		Mean $CaCO_3$ content (% of DW)	Live:dead rhodoliths	$CaCO_3$ (kg m^{-2})	Area (m^2)	$CaCO_3$ (kilotons)	Reference (area)
	Living	Dead						
Galway	3.1 (±1.2)	1.3 (±0.4)	92.3	2.6 (±1.1)	4.2 (±1.1)	-	-	-
Armação de Pêra	11.1 (±2.5)	2.1 (±1.2)	92.2	6.3 (±2.6)	12.7 (±3.0)	3000000	38.1	85
Porto Santo	29.0 (±6.1)	17.9 (±7.2)	97.6	2.1 (±1.4)	46.3 (±10.7)	101081	4.7	86
Madeira	15.7 (±4.8)	1.0 (±1.7)	95.6	41 (±36)	16.0 (±4.9)	28403	0.45	86
Gando	15.4 (±3.3)	24.3 (±4.3)	95.8	0.6 (±0.2)	39.1 (±6.1)	900000	35.2	87
Arguineguín	14.8 (±6.9)	1.8 (±1.7)	94.8	18 (±15)	15.9 (±7.0)	50000	0.79	Tuya (pers. comm.)
Taranto	11.7 (±1.6)	0.7 (±0.7)	92.3	35 (±34)	11.6 (±1.8)	50000	0.62	88
Sicily*	2.5 (±0.8)	1.7 (±0.6)	95.7	1.6 (±0.5)	4.1 (±1.2)	-	-	-
Arvoredo*	18.1 (±3.5)	3.5 (±1.6)	89.3	7.1 (±4.9)	19.9 (±2.3)	100000	2.2	89

For the latter, available estimates of the bed area were used. Data are mean (±SD).

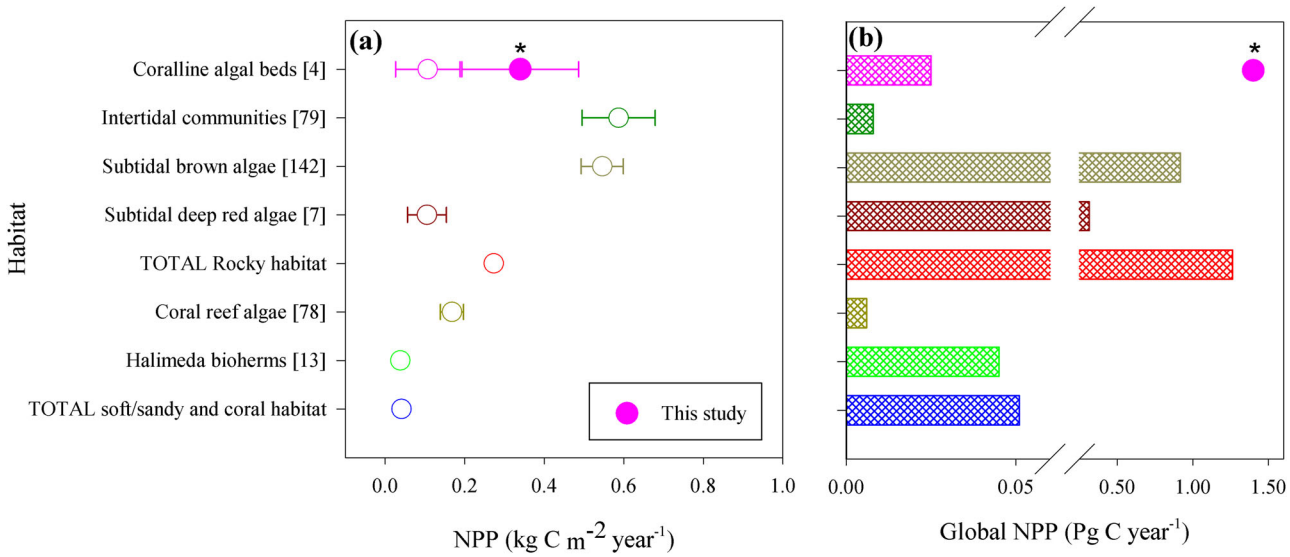

Fig. 4 | Comparison of net primary productivity (NPP) of macroalgal habitats. **a** Reported area-based net productivity[9] (*n* = indicated in brackets) and data obtained in this study (*summer only, *n* = 9 locations). Data are presented as means ± SE. **b** Estimated global productivity (in petagrams)[9], based on estimated global areas of the different habitats (for studied coralline algal beds, the global area estimate of 4.12 × 106 km^2 was used[21]) and mean NPP values (**a**).

Table 3 | Examples of productivity-associated carbon fluxes of calcifiers (CCA- crustose coralline algae) and their habitats (P- population-level estimations, C- community level estimations)

Calcifier/habitat	NPP	NCP	NPP:NCP	Net DIC flux	Reference
Coralline algal populations (P)	-5.2 –1650	1.9-349	-2.7 –4.7	↑6 –↓349	This study
Temperate coralline algal population (P)	-66 –53	2-126	-	↑67–23*	23
Mediterranean CCA (P)	14	23	0.6	↑0.2*	90
Tropical CCA (P)	14-109	8-91	1.1–2.8	↓9–72*	91,92
Temperate coralline algal bed (C)	-29 – -53	0.5–27	-	↑29–35*	24
Temperate coralline algal bed (C)	-	-	-	↓8.6	26
Mediterranean articulated coralline algae (C)	20	8	2.5	↓15*	20
Coral reef (C)	-0.4 –110	2.5–253	0.01-2.4	↑46 –↓80	Reviewed in[14]
	100	94	1.1	↓44*	93
	163	243	0.7	↑1.5	94
	-20 –110	190–200	-0.1 –0.6	↑4–140*	95
	100	390	0.3	↑134*	96
Algal-dominated reef (C)	8	0.8	10	↓10	17

Daily net primary (NPP) and carbonate productivity (NCP) estimates (mmol C uptake or mmol $CaCO_3$ m^{-2} day^{-1}), their ratios (NPP:NCP), and estimated net DIC flux dynamics. Data shown are means or ranges (↑- C release, ↓ - C uptake, *estimated by using $\Psi = 0.6$ to account for CO_2 release associated to carbonate production).

in the coral reef estimates; Table 3). Depending on its composition, the associated community contributes differently to the net carbon fluxes, which may cause shifts in NPP:NCP ratios, as illustrated by the large differences in the NPP:NCP ratios and net carbon fluxes of coral reefs versus algal-dominated reefs (Table 3). Our estimated ratios are likely to be higher in cases where the coralline algal bed harbors a large amount of rhodolith-associated algae, due to their contribution to the community NPP[29]. On the other hand, a high abundance of fauna in coralline algal beds might lead to lower NPP:NCP, due to higher respiratory carbon release, as demonstrated by the lower NPP estimates of a temperate coralline algal community with large faunal biomass[24], compared to higher values when considering only their rhodolith population[23] (see Table 3).

Coralline algal productivity also expressed a large variability among beds, which was strongly driven by in situ light availability, with a low contribution of temperature. This is consistent with previous findings of a depth-related decrease in productivity for *Lithothamnion corallioides* from the Bay of Brest, France[23]. In contrast, recent global models pointed towards a higher contribution of temperature to macroalgal habitats' NPP, while light had a rather low contribution[3]. This discrepancy might be related to the type of habitat analyzed (e.g., intertidal and subtidal marine forests, algal turfs) that encompassed a broader biogeographical range, but also to the use of irradiance derived from satellite data in the models, instead of in situ irradiance based on measured K_{PAR}. The latter can vary greatly among locations, e.g. with higher K_{PAR} at very shallow coastal locations (see Supplementary Fig. 2). Moreover, rhodolith species composition is also a contributing factor to the observed high variability in productivity among beds, as the species can exhibit strong differences in net productivity (primary and carbonate production) and hence, associated carbon uptake/release. This finding is consistent with evidence provided by other studies, showing that large differences exist among rhodolith species regarding their maximum physiological performance, the ratio of photosynthesis to calcification, and nighttime calcification rates[27,28].

Our study also provides an inventory of substantial, but highly variable $CaCO_3$ deposits in coralline algal beds (Table 2). While carbonate productivity of the respective coralline algal communities might have some influence, the occurrence of either dense or sparse accumulations of rhodoliths and hence, carbonate deposits in specific locations and depths, is mainly driven by local shelf morphology and hydrodynamic processes, such as wave-induced turbulence[49,50]. Likewise, the size of the carbonate deposits is also influenced by the thickness of the coralline algal bed, which has been shown to express a large variability, ranging from a single to multiple layers of rhodoliths, with reported values of 25 cm to 2 m in Northern European beds[51,52]. Similarly, a thickness of several meters has been reported in the Gulf of California, mainly formed by dead algal nodules/fragments, while living rhodolith thalli form 2–20 cm thick surface layers[53]. In our study, high but also largely variable amounts of $CaCO_3$ were found (4–46 kg m^{-2}). Similar values and variability have been reported for coralline algal beds along the Brazilian coast[54], with values ranging between 15 and 35 kg m^{-2}, in the Bay of Brest, France[55], with values ranging between 1.8 and 14.5 kg m^{-2}, and in the Mediterranean[56] 20.4 kg m^{-2} have been reported. This large variability, together with the large range of areal extensions of the studied coralline algal beds, resulted in a large range of the amounts of carbonate contained in the beds (0.4–38 kilotons). At present, this kind of information is extremely scarce, due to the lack of information on $CaCO_3$ deposits and areal extensions of coralline algal beds, but a similar value has been reported from a coralline algal bed in the Tyrrhenian Sea, Mediterranean[56], with 2.85 kilotons (bed size ~ 14 km^2).

Our data further indicate that coralline algal beds vary greatly in the amount of accumulated dead calcareous thalli/nodules, with ratios of live:dead rhodoliths ranging between 0.6 and 41. These values fall within the similar highly variable range of ratios reported from Atlantic North West Spain (0.2–99)[57], in the Bay of Brest (25–78)[58], in the Mediterranean (1–78)[59–61], while in California ratios between 1 and 5 have been reported[62]. The dissolution of the $CaCO_3$ contained in the dead algal nodules/thalli, due to bioerosion, microbial respiration and/or underlying sediment redox potential, is a component that has so far not been considered in coralline algal-bed associated carbon flux dynamics. By estimating $CaCO_3$ dissolution rates of dead algal nodules/thalli, and using simple stoichiometry of CO_2 removed from the seawater due to dissolution (i.e., $\Psi = 0.6$ mol)[63,64], our results indicate that in coralline algal beds with a high proportion of dead thalli, the dissolution can partially offset the calcification-association CO_2 release (e.g., by ~50% in Gando; Table 1). Moreover, the currently increasing anthropogenic CO_2 emissions, and related future projections, will likely change the contribution of the $CaCO_3$ production/dissolution dynamics on the net carbon fluxes of these habitats, though not in a straightforward manner. Ocean acidification will not only decrease coralline algal calcification[65], but also accelerate the dissolution of their dead skeletons, either directly due to the lower pH[36,66] or indirectly due to its effect on bioeroders[67]. On the other hand, the projected increase in Ψ with increasing atmospheric pCO_2

https://doi.org/10.1038/s41467-024-52697-5

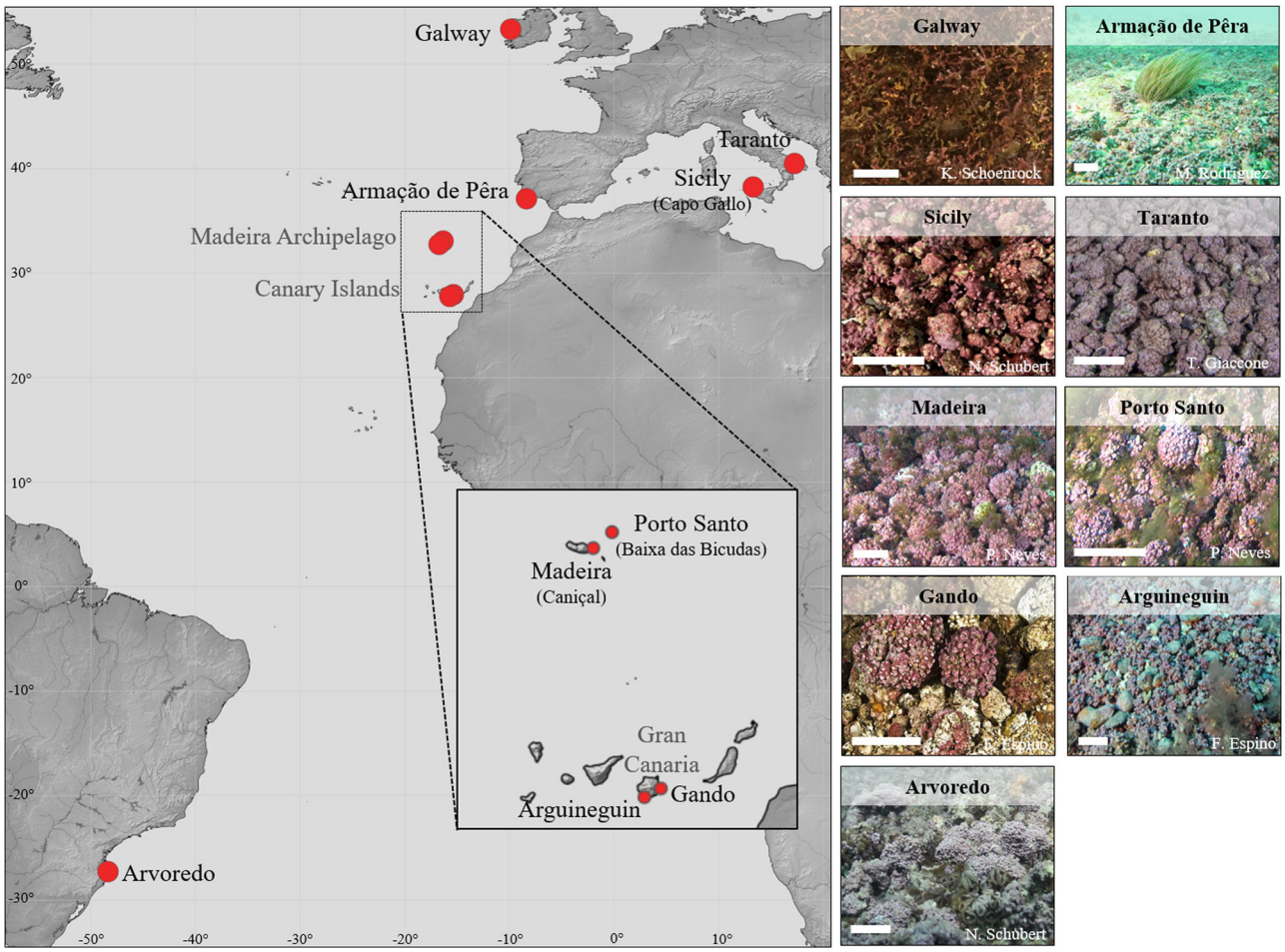

Fig. 5 | Sampling sites across the Atlantic and the Mediterranean. Map shows the coralline algal bed locations where rhodoliths were sampled and photos show the respective rhodolith communities (photos, white scale indicates 5 cm).

and temperature (e.g., from 0.6 to 0.72 and 0.84 at 500 ppm and 1000 ppm, respectively)[13,64] will have opposing effects on the $CaCO_3$-pump associated CO_2 fluxes, i.e. projected decrease in calcification will be associated with higher CO_2 release, while increased dissolution will remove higher amounts of CO_2 from the water column.

Understanding the oceanic carbon cycle, and its importance in the global carbon budget, requires in-depth knowledge of the associated carbon source/sink dynamics, such as those associated with the biological and $CaCO_3$ pump. Yet, large knowledge gaps persist, regarding the productivity and carbon fluxes associated with major marine habitats, e.g. those built by macroalgae and calcifiers. Recently, sound arguments for the large carbon uptake and sequestration capacity of macroalgal forests have been brought forward, based on their vast areal extent and high productivity[3,4,8,9]. Here, we expand this call of attention to coralline algal beds, based on their substantial global area extension[21], high productivity and associated carbon uptake, as well as their significant $CaCO_3$ deposits.

Our study represents an advancement towards a better understanding of the important role of coralline algal beds in the oceanic carbon cycle, despite some limitations. The here used organism-level approach provided only snap-shot summer productivity estimates for the coralline algal populations of the beds. Thus, an important next step will be to collect seasonal in situ productivity estimates (population- and ecosystem-level), to calculate annual budgets for the habitats' productivity and associated carbon flux dynamics. Furthermore, in order to obtain meaningful global estimates and to identify general patterns and drivers, e.g. influence of environmental factors and associated community, it is essential to augment the number of data sets, including a wide bathymetric and geographical scale. This, together with increasing efforts to resolve the areal extent and depth distribution of coralline algal beds at high resolution, will allow quantifying the absolute magnitude and direction of their associated carbon fluxes and carbonate deposits, as well as allowing to project potential changes in the future, as the oceans continue to warm and absorb anthropogenic CO_2 emissions.

Methods

Study sites and sampling

Rhodolith samples were collected from nine coralline algal beds (2–51 m depth) at the Northeastern Atlantic coast, in the Mediterranean, off the coast of northwestern Africa and in southern Brazil, by SCUBA diving during the warm season, i.e. early to late summer (Fig. 5, Supplementary Table 2). Immediately after collection, samples kept in coolers with seawater were transported to a nearby laboratory facility. For the duration of the experiments (1–3 days), the rhodoliths were kept in tanks (V = 60–100 L) with circulating seawater, at the temperature recorded during sampling and at the light intensity recorded at the collection depth (Supplementary Table 2).

Species identification

Atlantic rhodolith species were identified, as described[28], and included: *Phymatolithon calcareum* (Ireland), *P. lusitanicum* (South Portugal), the conspecific *Phymatolithon* sp. (Madeira and Canary Islands) and *Roseolithon crispatum* (as *Lithothamnion crispatum*), *Melyvonnea erubescens* and *Lithophyllum atlanticum* from South Brazil (Supplementary Table 1). Specimens of the Mediterranean species

Neogoniolithon brassica-florida (Taranto), and *Lithophyllum racemus, Lithothamnion* sp. and *Spongites* sp. (Sicily), used for the physiological measurements, were identified *a posteriori*, based on molecular tools. As *Lithothamnion* sp. and *Spongites* sp. were visually indistinguishable, a combination of specimens of both were used in the measurements and the data pooled together. For the identification, DNA was extracted from the 15 specimens from both Mediterranean locations (5 from Taranto and 10 from Sicily), using a E.Z.N.A.® Tissue DNA Kit (Omega Bio-tek, United States) following the manufacturer protocol. The psbA locus was amplified, using primer pairs: psbA-F1 (ATGACTGCTACTTTAGAAAGACG, primer sequence 5′-3′)/psbA-R1 (GCTAAATCTARWGGGAAGTTGTG, primer sequence 5′-3′)[68] and the thermal profile for amplification and PCR reaction followed[69]. The PCR product was purified and sequenced by the SAI-UBM department of the University of Coruña, Spain. Sequences were assembled with the assistance of CodonCode Aligner® (CodonCode Corporation, USA), adjusted by eye using SeaView version 4[70], and submitted to the Barcode of Life Data Systems (BOLD)[71] and GenBank. Sequences generated in the present study were compared with publicly available sequences for this group of red algae in GenBank (~7300 sequences). Estimates of genetic distance (uncorrected p-distances and number of base pair difference) were calculated in MEGA v. 6[72]. The low pairwise sequence divergence between the psbA sequences generated in the present study and publicly available sequences resulted in the identification of *Neogoniolithon brassica-florida* in Taranto (0–0.8-%; 0–6 bp difference with Gb acc. no. sequences JQ896257, FJ361443, and FJ361401) and *Lithophyllum racemus* in rhodoliths of Sicily (0–0.4 %; 0–3 bp difference with the neotype, GB acc. no. MT325777[73]). The remaining five rhodoliths collected from Sicily were temporarily identified as genus level: two rhodoliths were identified as *Lithothamnion* sp. based on the low divergence found with another *Lithothamnion* sp. (0.4–0.5%; 3-4 bp difference with *Lithothamnion* sp. from Vulcano Island, Italy, Gb acc. no. MZ438379[74]). The remaining three specimens were identified as *Spongites* sp., due to the high interspecific divergence found with any publicly available sequence provided for species of this genus (> 3.8%, 30 bp difference), including the Mediterranean *Spongites fruticulosus* (>5%, 40 bp difference with the sequence GB acc. n° MT325755 conspecific with the epitype of this species[74,75]).

Rhodolith biomass, carbonate content and carbonate standing stocks

For biomass determinations, rhodoliths were collected either using ten randomly placed quadrats (25 × 25 cm) or, in case of beds with multiple rhodolith layers (>10 cm thickness, i.e. Porto Santo and Arguineguín), by a PVC corer (Ø 11 cm), collecting the uppermost 10 cm (n = 10 cores). Each quadrat (or core) sample was bagged and brought back to the laboratory, where the samples were separated into dead (distinguishably gray or white colored) and living rhodoliths. In Brazilian and Sicilian coralline algal beds (dominated by multiple species) samples were further separated into the different species using morphological characteristics. All samples were oven-dried at 60 °C, for at least 48 h, and weighted for dry weight (DW) determination.

To determine the amount of carbonate per m^2 of coralline algal bed, for the living rhodolith component, which also contains a non-carbonate fraction (mainly organic matter), the amount of carbonate was estimated in subsamples. Specifically, a subsample ($n = 5$) of living samples per site and species were dried at 60 °C and weighted, decalcified with 2 M HCl, washed with distilled water, dried again at 60 °C, and weighted. The change in weight of the rhodoliths was calculated to be the carbonate content of an individual as a % of DW, which was then extrapolated to calculate the amount of $CaCO_3$ of the living rhodolith component as kg m^{-2}. In addition, the dry weight of the dead rhodolith proportion was considered to be composed of 100% $CaCO_3$ (DW = $CaCO_3$ content), as previous decalcification tests showed that the contribution of other material (e.g., sand, shells) was minimal (<1%). Both carbonate components were then added to obtain the total amount of $CaCO_3$ per m^2 of coralline algal bed.

Light conditions at the sampling sites

Daily light availability and variation at the different coralline algal beds were obtained, using light attenuation coefficients (K_{PAR}) measurements and incident light data, recorded at the different sites during sampling (Supplementary Fig. 2). K_{PAR} was obtained through in situ measurements of light profiles in the water column ($n = 5–6$ per site) during sample collection, using an underwater quantum sensor (LI-192, LI-COR Environmental, USA), attached to a LI-250A Light Meter (LI-COR Environmental, USA). In the case of the southern Brazilian site, a region influenced by strong coastal upwelling associated with frequent and strong winds, reported mean summer K_{PAR} values were used[76]. In addition, a light data logger (Odyssey, Dataflow Systems Pty Ltd, New Zealand), calibrated against a quantum sensor (LI-192, LI-COR Environmental, USA) attached to a LI-1400 data logger (LI-COR Environmental, USA), was used to record the incident light during the sampling week. For other sites, such as Galway and Arvoredo, available records were used from continuous recordings of incident irradiance (μmol photons m^{-2} s^{-1}), measured on the roof of the Martin Ryan Building, NUI Galway, using a LI-100 Light datalogger (LI-COR Environmental, USA), and from the Company of Agricultural Research and Rural Extension of Santa Catarina[77], respectively.

Rhodolith photosynthesis and calcification

Rhodolith individuals from each site ($n = 5$ per species and site; 3–4 cm in diameter), carefully cleaned with a toothbrush to remove epiphytes, were incubated with filtered seawater (0.45 μm) in sealed custom-made water-jacketed plexiglass chambers ($V = 150$ mL), with internal mixing provided by a magnetic stirrer. Temperature during incubation was set to the temperature recorded during collection (Supplementary Table 2) and controlled by connecting the external water jacket to a temperature-controlled water bath. After an initial incubation in darkness to determine dark respiration rates (R), rhodoliths were exposed to a series of increasing light intensities. The incubation time at each light intensity varied between 0.5 h for the Brazilian species, to 1 h for the other species. This was based on previous incubations, testing different times, to ensure a high enough signal-to-noise ratio for the measured parameters. At the beginning and end of each incubation, water samples were taken, poisoned with $HgCl_2$, and stored in borosilicate tubes (two tubes per incubation chamber, $V = 25$ mL each) for total alkalinity (TA) analyses. Afterwards, rhodoliths were dried (48 h at 60 °C) and their dry weight was used to normalize metabolic and calcification rates.

The calcification rates of the rhodolith species were determined using TA measurements of seawater samples before and after each incubation. For TA measurements, duplicate analyses of each sample were performed, using the Gran titration method[78,79]. The samples were titrated with HCl 0.1 M, using an automated titration system (Titroline 7000, SI Analytics, Mainz, Germany), coupled to an autosampler (TW alpha plus, SI Analytics, Mainz, Germany). Data were digitally captured and processed using Titrisoft 3.2 software (SI Analytics, Mainz, Germany). For quality control, a certified reference material of known total alkalinity was used to calibrate the method (CRMs, supplied by the Marine Physical Laboratory, Scripps Institution of Oceanography, USA). Similarly, at each site, dead rhodoliths were collected and incubated for 3–4 h, under dim-light conditions ($n = 5$ per site), as described above, to determine carbonate dissolution rates.

Data analysis

Biomass-specific net photosynthesis (Pn), respiration (R), and calcification (G), at each light intensity, were calculated through the

difference between initial and final concentrations[23]. From those data, the maximum photosynthetic and calcification rates (Pn_{max}, G_{max}) were obtained from the average of the maximum values above saturating irradiance, while the quantum efficiency (α) for each parameter was estimated from the initial slope of the light response curve by linear least-squares regression.

To quantify $CaCO_3$ precipitation and dissolution, total dissolved inorganic carbon fluxes (DIC flux) and carbon fluxes associated with net photosynthetic and respiration rates, the pH-TA technique was used[80,81]. DIC concentrations were estimated using the Excel macro CO2SYS[82], with pH, TA, temperature and salinity as inputs. Setting in CO2SYS were set to the NBS pH scale and the constants from Mehrbach et al. (1973), refit by Dickson and Millero (1987)[82]. Calcification and dissolution rates were determined by the total alkalinity-anomaly technique[80]. Considering that TA and DIC decrease by 2 mol and 1 mol, respectively, per mol of $CaCO_3$ precipitated, the change in DIC, associated to calcification (G), was then subtracted from ΔDIC to provide an estimate of the inorganic carbon uptake related to net primary production (Pn).

$$G\,(\mu mol\,CaCO_3\,g^{-1}\,DW\,h^{-1}) = (\Delta TA^{*}V)/(2^{*}DW^{*}t) \quad (1)$$

$$DIC\ flux\,(\mu mol\,C\,g^{-1}\,DW\,h^{-1}) = [(\Delta DIC^{*}V)/(DW^{*}t)] \quad (2)$$

$$Pn\ or\ R\,(\mu mol\,C\,g^{-1}\,DW\,h^{-1}) = DIC\ flux - G \quad (3)$$

where ΔDIC (μmol L^{-1}) and ΔTA (meq. L^{-1}) are the changes in the concentration of DIC and total alkalinity during the incubation, respectively, V is the chamber volume (L), t is the incubation time, and DW is the dry weight of the rhodolith (g).

Daily integrated (24 h) productivity was calculated using the in situ daily irradiance at the respective sampling site, averaged over the sampling week (see Supplementary Fig. 2), and the photosynthetic or calcification efficiency (α) and maximum net photosynthetic or calcification rate from the measured light curves (Supplementary Fig. 3, Supplementary Table 1). Daily net primary production (NPP) and net carbonate production (NCP) was obtained by integrating the net photosynthesis or light calcification during daytime (12–14 h, depending on site and date) and the dark respiration or dark calcification during the night-time period (10–12 h, depending on site and date). Subsequently, the living rhodolith biomass (g DW m^{-2}) of the respective coralline algal bed was used to calculate daily productivity of the rhodolith populations, NPP_P and NCP_P (m^{-2} coralline algal bed). Similarly, the biomass of dead rhodoliths and their respective dissolution rates (24 h) were used to calculate the daily carbonate dissolution of the different beds and the associated CO_2 removal. The latter was obtained, using a Ψ (psi, released CO_2/precipitated carbonate) determined in seawater of 0.6[63,64].

To test if and to which degree the daily in situ light and temperature conditions, at the different coralline algal beds, contributed to the variation in NPP and NCP, Generalized Additive Models (GAMs) were fitted using the mgcv R package[83]. All models were fitted through a Poisson family error structure and a log link function, with the basis dimensions of the smooth terms (thin plate regression splines) limited to 3 knots to avoid overfitting and ensure monotonic relationships. We checked for normality and homoscedasticity of model residuals through visual examination.

Separately, after testing for normality and heteroscedasticity, using the Shapiro-Wilk and Levene's tests, respectively, one-way ANOVAs were used to test for significant differences in productivity rates of *Phymatolithon* sp. from different Lusitanian (Madeira, Porto Santo, Gran Canaria, *sensu*[84]) coralline algal beds, as well as for differences among the three species dominating the Brazilian bed.

Reporting summary

Further information on research design is available in the Nature Portfolio Reporting Summary linked to this article.

Data availability

The authors declare that all data supporting the findings of this study are available within the paper and its supplementary information files. The nucleotide sequences of the psbA genes from the here identified species have been deposited in GenBank under the accession numbers PQ299081–PQ299095.

References

1. Friedlingstein, P. et al. Global carbon budget 2023. *Earth Syst. Sci. Data* **15**, 5301–5369 (2023).
2. DeVries, T. The ocean carbon cycle. *Ann. Rev. Env. Resour.* **47**, 317–341 (2022).
3. Pessarrodona, A. et al. Global seaweed productivity. *Sci. Adv.* **8**, eabn2465 (2022).
4. Pessarrodona, A. et al. Carbon sequestration and climate change mitigation using macroalgae: a state of knowledge review. *Biol. Rev.* **98**, 1945–1971 (2023).
5. Pessarrodona, A., Moore, P. J., Sayer, M. D. J. & Smale, D. A. Carbon assimilation and transfer through kelp forests in the NE Atlantic is diminished under a warmer ocean climate. *Global Change Biol* **24**, 2486–2498 (2018).
6. Watanabe, K. et al. Macroalgal metabolism and lateral carbon flows can create significant carbon sinks. *Biogeosciences* **17**, 2425–2440 (2020).
7. Filbee-Dexter, K. et al. Seaweed forests are carbon sinks that may help mitigate CO_2 emissions: a comment on Gallagher et al. (2022). *ICES J. Mar. Sci.* **80**, 1814–1819 (2023).
8. Pessarrodona, A. et al. A global dataset of seaweed net primary productivity. *Sci. Data* **9**, 484 (2022).
9. Duarte, C. M. et al. Global estimates of the extent and production of macroalgal forests. *Global Ecol. Biogeogr.* **31**, 1422–1439 (2022).
10. Macreadie, P. I., Serrano, O., Maher, D. T., Duarte, C. M. & Beardall, J. Addressing calcium carbonate cycling in blue carbon accounting. *Limnol. Oceanogr. Lett.* **2**, 195–201 (2017).
11. Raven, J. Blue carbon: past, present and future, with emphasis on macroalgae. *Biol. Lett.* **14**, 20180336 (2018).
12. Raven, J. A. & Falkowski, P. G. Oceanic sinks for atmospheric CO_2. *Plant, Cell & Env* **22**, 741–755 (1999).
13. Smith, S. V. Parsing the oceanic calcium carbonate cycle: a net atmospheric carbon dioxide source or a sink? *Assoc. Sci. Limnol. Oceanogr*. https://doi.org/10.4319/svsmith.2013.978-0-9845591-2-1 (2013).
14. Suzuki, A. & Kawahata, H. Carbon budget of coral reef systems: an overview of observations in fringing reefs, barrier reefs and atolls in the Indo-Pacific regions. *Tellus* **55B**, 428–444 (2003).
15. Kayanne, H., Suzuki, A. & Saito, H. Diurnal changes in the partial pressure of carbon dioxide in coral reef water. *Science* **269**, 214–216 (1995).
16. Gattuso, J.-P., Pichon, M. & Frankignoulle, M. Biological control of air-sea CO_2 fluxes: effect of photosynthetic and calcifying marine organisms and ecosystems. *Mar. Ecol. Prog. Ser.* **129**, 307–312 (1995).
17. Gattuso, J.-P., Payri, C. E., Pichon, M., Delesalle, B. & Frankignoulle, M. Primary production, calcification, and air-sea CO_2 fluxes of a macroalgal-dominated coral reef community (Moorea, French Polynesia). *J. Phycol.* **33**, 729–738 (1997).
18. Suzuki, A. Combined effects of photosynthesis and calcification on the partial pressure of carbon dioxide in seawater. *J. Oceanogr.* **54**, 1–7 (1998).
19. Mazarrasa, I. et al. Seagrass meadows as a globally significant carbonate reservoir. *Biogeosciences* **12**, 4993–5003 (2015).

20. Bensoussan, N. & Gattuso, J.-P. Community primary production and calcification in a NW Mediterranean ecosystem dominated by calcareous macroalgae. *Mar. Ecol. Prog. Ser.* **334**, 37–45 (2007).
21. Fragkopoulou, E., Serrão, E. A., Horta, P. A., Koerich, G. & Assis, J. Bottom trawling threatens future climate refugia of rhodoliths globally. *Front. Mar. Sci.* **7**, 594537 (2021).
22. Tuya, F. et al. Levelling-up rhodolith-bed science to address global-scale conservation challenges. *Sci. Total Env.* **892**, 164818 (2023).
23. Martin, S., Castets, M.-D. & Clavier, J. Primary production, respiration and calcification of the temperate free-living coralline alga *Lithothamnion corallioides*. *Aquat. Bot.* **85**, 121–128 (2006).
24. Martin, S., Clavier, J., Chauvaud, L. & Thouzeau, G. Community metabolism in temperate maerl beds. I. carbon and carbonate fluxes. *Mar. Ecol. Prog. Ser.* **335**, 19–29 (2007).
25. Attard, K. M. et al. Benthic oxygen exchange in a live coralline algal bed and an adjacent sandy habitat: an eddy covariance study. *Mar. Ecol. Prog. Ser.* **535**, 99–115 (2015).
26. Martin, S. et al. Comparison of *Zostera marina* and Maerl community metabolism. *Aquat. Bot.* **83**, 161–174 (2005).
27. Qui-Minet, Z. N. et al. Physiology of maerl algae: comparison of inter-and intraspecies variations. *J. Phycol.* **57**, 831–848 (2021).
28. Schubert, N. et al. Rhodolith physiology across the Atlantic: towards a better mechanistic understanding of intra- and interspecific differences. *Front. Mar. Sci.* **9**, 921639 (2022).
29. Qui-Minet, Z. N., Davoult, D., Grall, J. & Martin, S. The relative contribution of fleshy epiphytic macroalgae to the production of temperate maerl (rhodolith) beds. *Mar. Ecol. Prog. Ser.* **693**, 69–82 (2022).
30. Kempf, M. Notes on the benthic bionomy of the N-NE Brazilian shelf. *Mar. Biol.* **5**, 213–224 (1970).
31. Milliman, J. D. & Amaral, C. A. Economic potential of Brazilian continental margin sediments. *Annals of 28th Braz. Congr. Geol.* 1, 335–344 (1974).
32. van der Heijden, L. H. & Kamenos, N. A. Reviews and syntheses: calculating the global contribution of coralline algae to total carbon burial. *Biogeosciences* **12**, 6429–6441 (2015).
33. Elderfield, H. Carbonate mysteries. *Science* **296**, 1618–1621 (2002).
34. Mao, J. et al. Carbon burial over the last four millennia is regulated by both climatic and land use change. *Global Change Biol* **26**, 2496–2504 (2020).
35. Andersson, A. J., Mackenzie, F. T. & Lerman, A. Coastal ocean and carbonate systems in the high CO_2 world of the Anthropocene. *Am. J. Sci.* **305**, 918 (2005).
36. Kamenos, N. A. et al. Coralline algal structure is more sensitive to rate, rather than the magnitude, of ocean acidification. *Global Change Biol* **19**, 3621–3628 (2013).
37. Andersson, A. J., Bates, N. R. & Mackenzie, F. T. Dissolution of carbonate sediments under rising pCO_2 and ocean acidification: observations from devil's hole. *Bermuda. Aquat. Geochem.* **13**, 237–264 (2007).
38. Andersson, A. J. & Gledhill, D. K. Ocean acidification and coral reefs: effects of breakdown, dissolution, and net ecosystem calcification. *Annu. Rev. Mar. Sci.* **5**, 321–348 (2013).
39. Eyre, B. D. et al. Coral reefs will transition to net dissolving before end of century. *Science* **359**, 908–911 (2018).
40. Rodgers, K. L. & Shears, N. T. Modelling kelp forest primary production using in situ photosynthesis, biomass and light measurements. *Mar. Ecol. Prog. Ser.* **553**, 67–79 (2016).
41. White, L., Loisel, S., Sevin, L. & Davoult, D. In situ estimates of kelp forest productivity in macro-tidal environments. *Limnol. Oceanogr.* **66**, 4227–4239 (2021).
42. Franke, K., Matthes, L. C., Graiff, A., Karsten, U. & Bartsch, I. The challenge of estimating kelp production in a turbid marine environment. *J. Phycol.* **59**, 518–537 (2023).
43. Kim, J. H. et al. Assessing photosynthetic uptake of total inorganic carbon in an *Ecklonia cava* dominated seaweed artificial reef: population-and community-level metabolisms. *J. Appl. Phycol.* **36**, 969–981 (2024).
44. Naumann, M. S., Jantzen, C., Haas, A. F., Iglesias-Prieto, R. & Wild, C. Benthic primary production budget of a Caribbean reef lagoon (Puerto Morelos, Mexico). *PLoS ONE* **8**, e82923 (2013).
45. Owen, D. P., Long, M. H., Fitt, W. K. & Hopkinson, B. M. Taxon-specific primary production rates on coral reefs in the Florida keys. *Limnol. Oceanogr.* **66**, 625–638 (2021).
46. Gattuso, J.-P., Frankignoulle, M. & Wollast, R. Carbon and carbonate metabolism in coastal aquatic ecosystems. *Ann. Rev. Ecol. Syst.* **29**, 405–434 (1998).
47. Gattuso, J.-P., Frankignoulle, M. & Smith, S. V. Measurement of community metabolism and significance in the coral reef CO_2-source-sink debate. *Proc. Natl. Acad. Sci. USA* **96**, 13017–13022 (1999).
48. Cabrito, A., de Juan, S., Hinz, H. & Maynou, F. Morphological insights into the three-dimensional complexity of rhodolith beds. *Mar. Biol.* **171**, 127 (2024).
49. Marrack, E. C. The relationship between water motion and living rhodolith beds in the southwestern Gulf of California, Mexico. *PALAIOS* **14**, 159–171 (1999).
50. Ambrosio, B. G., Takase, L. S., Stein, L. P., Costa, M. B. & Siegle, E. Wave-induced sediment and rhodolith mobility on a narrow insular shelf dominated by wave variability (Fernando de Noronha Archipelago, Brazil). *Cont. Shelf Res.* **235**, 104662 (2022).
51. Blunden, G., Farnham, W. F., Jephson, N., Fenn, R. H. & Plunkett, B. A. The composition of maerl from the Glenan Islands of southern Brittany. *Bot. Mar.* **20**, 121–125 (1977).
52. Porter, J. S. et al. Blue carbon audit of Orkney waters. *Scottish Mar. Freshw. Sci.* **11**, 1–86 (2020).
53. Foster, M. S., Riosmena-Rodríguez, R., Steller, D. L. & Woelkerling, W. J. Living rhodolith beds in the Gulf of California and their implications for palaeoenvironmental interpretation. In, *Pliocene Carbonates And Related Facies Flanking The Gulf Of California, Baja California, Mexico* (eds. Johnson, M. E. & Vázquez, J. L.) 127–139 (Geological Society of America, 1997).
54. Carvalho, V. F. et al. Environmental drivers of rhodolith beds and epiphytes community along the South western Atlantic coast. *Mar. Environ. Res.* **154**, 104827 (2020).
55. Qui-Minet, Z. M. et al. The role of local environmental changes on maerl and its associated non-calcareous epiphytic flora in the Bay of Brest. *Est. Coast. Shelf Sci.* **208**, 140–152 (2018).
56. Savini, A., Basso, D., Bracchi, V. A. & Corselli, C. Maerl-bed mapping and carbonate quantification on submerged terraces offshore the Cilento peninsula (Tyrrhenian Sea, Italy). *Geodiversitas* **34**, 77–98 (2012).
57. Peña, V. & Bárbara, I. Maërl community in the north-western Iberian Peninsula: a review of floristic studies and long-term changes. *Aquat. Conserv. Mar. Freshw. Ecosyst.* **18**, 339–366 (2008).
58. Bernard, G. et al. Declining maerl vitality and habitat complexity across a dredging gradient: insights from in situ sediment profile imagery (SPI). *Sci. Rep.* **9**, 16463 (2019).
59. Bordehore, C., Ramos-Esplá, A. A. & Riosmena-Rodríguez, R. Comparative study of two maerl beds with different otter trawling history, southeast Iberian Peninsula. *Aquat. Conserv. Mar. Freshw. Ecosyst.* **13**, S43–S54 (2003).
60. Chimienti, G. et al. Rhodolith beds heterogeneity along the Apulian continental shelf (Mediterranean Sea). *J. Mar. Sci. Eng.* **8**, 813 (2020).
61. Rendina, F. et al. Distribution and characterization of deep rhodolith beds off the Campania coast (SW Italy, Mediterranean Sea). *Plants* **9**, 985 (2020).

62. Tompkins, P. A. & Steller, D. L. Living carbonate habitats in temperate California (USA) waters: distribution, growth, and disturbance of Santa Catalina island rhodoliths. *Mar. Ecol. Prog. Ser.* **560**, 135–145 (2016).
63. Ware, J. R., Smith, S. V. & Reaka-Kudla, M. L. Coral reefs: sources or sinks of atmospheric CO_2? *Coral Reefs* **11**, 127–130 (1992).
64. Frankignoulle, M., Canon, C. & Gattuso, J.-P. Marine calcification as a source of carbon dioxide: positive feedback of increasing atmospheric CO_2. *Limnol. Oceanogr.* **39**, 458–462 (1994).
65. Martin, S. & Hall-Spencer, J. M. Effects of ocean warming and acidification on rhodolith/mäerl beds. In *Rhodolith/Mäerl Beds: A Global Perspective*, (eds. Rodríguez, R. R., Nelson, W. & Aguirre, J.) 55–85 (Springer International Publishing, Switzerland, 2017).
66. Reyes-Nivia, C., Diaz-Pulido, G. & Dove, P. M. Relative roles of endolithic algae and carbonate chemistry variability in the skeletal dissolution of crustose coralline algae. *Biogeosciences* **11**, 4615–4626 (2014).
67. Schönberg, C. H., Fang, J. K., Carreiro-Silva, M., Tribollet, A. & Wisshak, M. Bioerosion: the other ocean acidification problem. *ICES J. Mar. Sci.* **74**, 895–925 (2017).
68. Yoon, H. S., Hackett, J. D. & Bhattacharya, D. A single origin of the peridinin- and fucoxanthin-containing plastids in dinoflagellates through tertiary endosymbiosis. *Proc. Nat. Acad. Sci. USA* **99**, 11724–11729 (2002).
69. Peña, V. et al. An integrative systematic approach to species diversity and distribution in the genus *Mesophyllum* (Corallinales, Rhodophyta) in Atlantic and Mediterranean Europe. *Eur. J. Phycol.* **50**, 20–36 (2015).
70. Gouy, M., Guindon, S. & Gascuel, O. SeaView Version 4: a multiplatform graphical user interface for sequence alignment and phylogenetic tree building. *Mol. Biol. Evol.* **27**, 221–224 (2010).
71. Ratnasingham, S. & Hebert, P. D. N. The barcode of life data system. *Mol. Ecol. Notes* **7**, 355–364 (2007).
72. Tamura, K., Stecher, G., Peterson, D., Filipski, A. & Kumar, S. MEGA6: Molecular evolutionary genetics analysis version 6.0. *Mol. Biol. Evol.* **30**, 2725–2729 (2013).
73. Caragnano, A. et al. Circumscription of *Lithophyllum racemus* (Corallinales, Rhodophyta) from the western Mediterranean sea reveals the species *Lithophyllum pseudoracemus* sp. nov. *Phycologia* **59**, 584–597 (2020).
74. Peña, V. et al. Major loss of coralline algal diversity in response to ocean acidification. *Global Change Biol* **27**, 4785–4798 (2021).
75. Rösler, A., Perfectti, F., Peña, V. & Braga, J. C. Phylogenetic relationships of Corallinaceae (Corallinales, Rhodophyta): taxonomic implications for reef-building corallines. *J. Phycol.* **52**, 412–431 (2016).
76. MAArE. *Projeto De Monitoramento Ambiental Da Reserva Biológica Marinha do Arvoredo E Entorno*. https://noticias.ufsc.br/ (2017).
77. EPAGRI. Empresa de Pesquisa Agropecuária e Extensão Rural de Santa Catarina. Banco de dados de variáveis ambientais de Santa Catarina. Florianópolis: 20p. (Epagri, Documentos, 310) - ISSN 2674-9521 (On-line) (2020).
78. Hansson, I. & Jagner, D. Evaluation of the accuracy of gran plots by means of computer calculations: application to the potentiometric titration of the total alkalinity and carbonate content in sea water. *Anal. Chim. Acta* **75**, 363–373 (1973).
79. Bradshaw, A. L., Brewer, P. G., Shafer, D. K. & Williams, R. T. Measurements of total carbon dioxide and alkalinity by potentiometric titration in the GEOSECS program. *Earth Planet. Sci. Lett.* **55**, 99–115 (1981).
80. Smith, S. V. & Key, G. S. Carbon dioxide and metabolism in marine environments. *Limnol. Oceanogr.* **20**, 493–495 (1975).
81. Smith, S. V. & Kinsey, D. W. Calcification and organic carbon metabolism as indicated by carbon dioxide. In, *Coral Reefs: Research Methods. Monographs On Oceanographic Methodology* (eds. Stoddart, D. & Johannes, R.) 581 (UNESCO, 1978).
82. Lewis, E. & Wallace, D. W. R. Program developed for CO_2 system calculations. *Tech. Rep*. https://doi.org/10.2172/639712 (1998).
83. Wood, S. & Wood, M. S. Package 'mgcv'. *R package version* **1**, 729 (2015).
84. Spalding, M. D. et al. Marine ecoregions of the world: a bioregionalization of coastal and shelf areas. *BioScience* **57**, 573–583 (2007).
85. Sordo, L., Santos, R., Barrote, I. & Silva, J. High CO_2 decreases the long-term resilience of the free-living coralline algae *Phymatolithon lusitanicum*. *Ecol. Evol.* **8**, 4781–4792 (2018).
86. Neves, P., Silva, J., Peña, V. & Ribeiro, C. Pink round stones'—rhodolith beds: an overlooked habitat in Madeira Archipelago. *Biodiv. Conserv.* **30**, 3359–3383 (2021).
87. Otero-Ferrer, F. et al. Early-faunal colonization patterns of discrete habitat units: a case study with rhodolith-associated vagile macrofauna. *Est. Coast. Shelf Sci.* **218**, 9–22 (2019).
88. Pierri, C. et al. Invertebrate diversity associated with a shallow rhodolith bed in the Mediterranean Sea (Mar Piccolo of Taranto, south-east Italy). *Aquat. Conserv. Mar. Freshw. Ecosyst.* **34**, e4054 (2024).
89. Gherardi, D. F. M. Community structure and carbonate production of a temperate rhodolith bank from Arvoredo Island, Southern Brazil. *Brazil. J. Oceanogr.* **52**, 207–224 (2004).
90. Martin, S., Charnoz, A. & Gattuso, J.-P. Photosynthesis, respiration and calcification in the Mediterranean crustose coralline alga *Lithophyllum cabiochae* (Corallinales, Rhodophyta). *Eur. J. Phycol.* **48**, 163–172 (2013).
91. Chisholm, J. R. W. Calcification by crustose algae on the northern Great Barrier Reef, Australia. *Limnol. Oceanogr.* **45**, 1476–1484 (2000).
92. Chisholm, J. R. W. Primary productivity of reef-building crustose coralline algae. *Limnol. Oceanogr.* **48**, 1376–1387 (2003).
93. Barnes, D. J. & Devereux, M. J. Productivity and calcification on a coral reef: a survey using pH and oxygen electrode techniques. *J. Exp. Mar. Biol. Ecol.* **79**, 213–231 (1984).
94. Gattuso, J.-P., Pichon, M., Delesalle, B. & Frankignoulle, M. Community metabolism and air-sea CO_2 fluxes in a coral reef ecosystem (Moorea, Franch Polynesia). *Mar. Ecol. Prog. Ser.* **96**, 259–267 (1993).
95. Falter, J. L., Lowe, R. J., Atkinson, M. J. & Cuet, P. Seasonal coupling and de-coupling of net calcification rates from coral reef metabolism and carbonate chemistry at Ningaloo Reef, Western Australia. *J. Geophys. Res: Oceans* **117**, C05003 (2012).
96. DeCarlo, T. M. et al. Community production modulates coral reef pH and the sensitivity of ecosystem calcification to ocean acidification. *J. Geophys. Res.* **122**, 745–761 (2017).

Acknowledgements

This research was supported by the EU Horizon 2020 research and innovation programs under the Marie Sklodowska-Curie Grant agreement No. 844703 (NS), by ASSEMBLE Plus project - Transnational Access #11154 (NS), through Portuguese National Funds from FCT-Fundação para a Ciência e a Tecnologia through Stimulus of Scientific Employment, Individual Support DOI:10.54499/2020.01282.CEECIND/CP1597/CT0003 (NS), through projects UIDB/04326/2020 (DOI:10.54499/UIDB/04326/2020) (NS, RS, JS), UIDP/04326/2020 (DOI:10.54499/UIDP/04326/2020) (NS, RS, JS), LA/P/0101/2020 (DOI:10.54499/LA/P/0101/2020) (NS, RS, JS), by a FCT/CAPES project 2019.00067.CBM (NS), by the Spanish Science and Innovation Ministry through the project 'POPCORN', PID2021-124257OB-I00 (FT, VP), by the British Phycological Society 2022-BPS-0117 (FR), by grants from FAPESC, FINEP/Rede CLIMA 01.13.0353-00 (PAH.) and CNPq-Universal 426215/2016-8 (PAH.). FR, GS, MCM acknowledge the project funded under the National Recovery and

Resilience Plan (NRRP), Mission 4 Component 2 Investment 1.4—Call for tender No. 3138 of 16 December 2021, rectified by Decree n.3175 of 18 December 2021 of Italian Ministry of University and Research funded by the European Union—NextGenerationEU. Project code CN_00000033, Concession Decree No. 1034 of 17 June 2022 adopted by the Italian Ministry of University and Research, CUP C63C22000520001 project National Biodiversity Future Center—NBFC, which supported the activities carried out in Sicily and Taranto. MCM and GS acknowledge the FEAMP Misura 1.40 - Accordo finalizzato alla mappatura e monitoraggio della biodiversità e valutazione dello stato ecologico degli habitat target all'interno dell'AMP Capo Gallo-Isola delle Femmine con particolare attenzione alle zone interessate dalla pesca - CUP: C73C23000240005 that supported the pre-survey that facilitated the sampling site selection in Sicily. MN has been supported by a PhD fellowship funded by the SZN (Open University – SZN PhD Program).

NS thanks intern Marie Brock for support with sample analysis, Maeve Edwards (National University of Galway) for her support with experiments, and Miguel Rodrigues (DiveSpot) and the AguaViva team for their support with the fieldwork at Armação de Pêra (Portugal) and in Arvoredo (Brazil), respectively. The authors thank the Museu da Baleia da Madeira for the logistical support during the sampling efforts in Caniçal, the Instituto das Florestas e Conservação da Natureza for house assistance in Porto Santo Island, and Estação de Biologia Marinha do Funchal for all the logistical support during the Madeira Island field campaigns. VP thanks Marie Marbaix (Museum national d´Histoire Naturelle) for their help with molecular work. Acquisition of part of the molecular data was carried out at the 'Service de Systématique Moléculaire', UMS 2700 2AD, MNHN, CNR. In the Canary Islands, rhodolith samples were collected under license n°SGPM/BDM/AUTSPP/5212019, provided by the General Sub-Directorate General for the Protection of the Sea (Ministry for the Ecological Transition and the Demographic Challenge- Spain). Sampling in the Arvoredo MPA (Brazil) was authorized by ICMBio (Instituto Chico Mendes de Conservação da Biodiversidade, #56981-1) and sampling in Taranto was authorized by the Comune di Taranto (Protocollo 0089698/2023 del 21/03/2023). For the sampling in Sicily, the authors thank the Italian Coast Guard management body of the Marine Protected Area of Capo Gallo Isola delle Femmine for granting the permission to perform the survey in the area, Antonino Scontrino and his team (Dive Center Saracen) for their support during fieldwork, and the researchers at the Laboratory of Ecology (Dipartimento di Scienze della Terra e del Mare, Università degli Studi di Palermo) for their support.

Author contributions

N.S. and J.S. conceived the study and designed the experiments. N.S., F.T., P.A.H., V.W.S., P.N., C.R., F.O.-F., F.E., K.S., F.R., I.O., T.G., M.N., M.F.T., F.P.M., and J.S. collected samples and field data. P.A.H., M.C.M., M.B.-B., G.S., R.S., and J.S. provided laboratory and logistic support. N.S., V.W.S., F.R., I.O., M.N., and J.S. performed experiments. V.P. and L.L.G. performed molecular identification. N.S. performed sample analysis. N.S., S.M. and F.T. performed data analysis. N.S. curated data and wrote the original draft. N.S., P.A.H., F.R., R.S., and J.S. provided financial support through project funds. All authors provided contributions to the final manuscript.

Competing interests

The authors declare no competing interests.

Additional information

Supplementary information The online version contains supplementary material available at https://doi.org/10.1038/s41467-024-52697-5.

Correspondence and requests for materials should be addressed to Nadine Schubert.

Peer review information *Nature Communications* thanks Guillermo Diaz-Pulido and Tessa Page for their contribution to the peer review of this work. A peer review file is available

Reprints and permissions information is available at http://www.nature.com/reprints

Publisher's note Springer Nature remains neutral with regard to jurisdictional claims in published maps and institutional affiliations.

[1]Centre of Marine Sciences (CCMAR/CIMAR LA), Campus de Gambelas, Universidade do Algarve, 8005-139 Faro, Portugal. [2]Grupo en Biodiversidad y Conservación (IU-ECOAQUA), Universidad de Las Palmas de Gran Canaria, Telde, Spain. [3]BioCost Research Group, Departamento de Bioloxía, Facultade de Ciencias, Universidade da Coruña, A Coruña, Spain. [4]Laboratório de Ficologia, Departamento de Botânica, Centro de Ciências Biológicas, Universidade Federal de Santa Catarina, Florianopolis, Brazil. [5]Observatório Oceânico da Madeira, Agência Regional para o Desenvolvimento da Investigação, Tecnologia e Inovação (OOM/ ARDITI), Edifício Madeira Tecnopolo, Funchal, Madeira, Portugal. [6]IFCN—Instituto das Florestas e Conservação da Natureza, IP-RAM, Madeira Funchal, Portugal. [7]Asociación Biodiversidad Atlántica y Sostenibilidad (ABAS), Telde, Spain. [8]Department of Zoology, School of Natural Sciences, The Ryan Institute for Environmental, Marine and Energy Research, University of Galway, Galway, Ireland. [9]Department of Integrative Marine Ecology, Stazione Zoologica Anton Dohrn, Genoa Marine Centre, Genova, Italy. [10]NBFC, National Biodiversity Future Center, Piazza Marina 61, 90133 Palermo, Italy. [11]Department of Integrative Marine Ecology, Stazione Zoologica Anton Dohrn, Naples, Italy. [12]Department of Integrative Marine Ecology (EMI), Anton Dohrn Zoological Station, Sicily Marine Centre, Messina, Italy. [13]Department of Integrative Marine Ecology (EMI), Stazione Zoologica Anton Dohrn, Sicily Marine Centre Lungomare Cristoforo Colombo (complesso Roosevelt), Palermo, Italy. [14]Laboratory of Ecology, Department of Earth and Marine Sciences, DiSTeM, University of Palermo, Palermo, Italy. [15]UMR 7144 Adaptation et Diversité en Milieu Marin, CNRS, Sorbonne Université, Station Biologique de Roscoff, Roscoff, France. [16]Institut de Systématique, Évolution, Biodiversité (ISYEB), Muséum National d'Histoire Naturelle, CNRS, Sorbonne Université, EPHE, Université des Antilles, Paris, France. [17]Present address: Melbourne Integrative Genomics, The University of Melbourne, Parkville, Australia. ✉e-mail: nadine_schubert@hotmail.com